Journal of Alloys and Compounds 614 (2014) 353–359

Contents lists available at ScienceDirect

Journal of Alloys and Compounds

journal homepage: www.elsevier.com/locate/jalcom

Synthesis of Bi_2O_3 architectures in DMF–H_2O solution by precipitation method and their photocatalytic activity

Li-Li Yang, Qiao-Feng Han *, Jin Zhao, Jun-Wu Zhu, Xin Wang *, Wei-Hua Ma

Key Laboratory for Soft Chemistry and Functional Materials, Ministry of Education, Nanjing University of Science and Technology, Nanjing 210094, China

ARTICLE INFO

Article history:
Received 9 March 2014
Received in revised form 31 May 2014
Accepted 2 June 2014
Available online 27 June 2014

Keywords:
Bi_2O_3
Precipitation method
Hierarchical architecture
Photodegradation

ABSTRACT

Well-crystalline flowerlike α-Bi_2O_3 hierarchical architectures with pineapple-shaped petals have been synthesized by precipitation method at a volume ratio of DMF/H_2O of 5, where DMF and H_2O were used to dissolve $Bi(NO_3)_3$ and KOH, respectively. If the DMF/H_2O ratio was decreased to 2:1, 1:1 and 0:30, flower-, bundle- and dendrite-shaped α-Bi_2O_3 microcrystallites aggregated by nanorods were formed, respectively. The simple synthetic route and thus obtained Bi_2O_3 architectures of various morphologies provide a basis insight for their formation mechanism. The photocatalytic activity of the as-prepared Bi_2O_3 particles for degradation of Rhodamine B (RhB) under visible-light irradiation was obviously influenced by their morphologies. Bi_2O_3 of nanorod-based microstructures exhibited higher photodegradation activity than nanobrick-based ones, owing to higher light absorption and carrier separation efficiency in one-dimensional (1D) nanostructured materials.

1. Introduction

Bismuth oxide (Bi_2O_3), a p-type semiconductor, is widely used as solid electrolyte in gas sensors [1–3], solid fuel cells [4–7], and photocatalysts [8–12]. As comparison to their bulk counterparts, nanostructured Bi_2O_3 have attracted more research interest due to the high surface area, exposed active lattice facets and thus excellent properties. For example, nanostructured Bi_2O_3 is considered as a good visible light photocatalyst candidate due to its narrow band gap (about 2.8 eV) and deep valence band comparable to that of TiO_2 [9,13]. More recently, nanostructured Bi_2O_3 has been used as composite photocatalysts and co-catalysts because Bi_2O_3 alone shows a low photocatalytic activity resulting from its more positive potential of the conduction band edge for the single-electron reduction of oxygen (E_{cb} = 0.33 V; $O_2 + e^- = O_2^-$, $E = -0.064$ V vs SHE) [14–16].

The design and synthesis of the three dimensional (3D) hierarchical architectures by self-assembly of nanostructured building components have received considerable attention in nanoscience and nanotechnology owing to shaped-dependent physical and chemical properties. Various Bi_2O_3 hierarchical architectures have been successfully synthesized. Zhou et al. prepared the Bi_2O_3 hierarchical architectures composed of 2D sheets via a template-free aqueous method in the presence of VO_3^- at 60–80 °C, which showed much higher photocatalytic activity over commercial Bi_2O_3 under visible light irradiation [8]. Hierarchical rippled Bi_2O_3 nanobelts were synthesized by an electrodeposition route and possessed higher specific capacitance and electrochemical stability as supercapacitor electrodes than nanobelts with smooth surface [17]. α-Bi_2O_3 microcrystals and microrods with pyramidal tips have been grown by a vapor–solid method using pure Bi as starting material [18]. Yu et al synthesized flower-like Bi_2O_3 superstructures with excellent visible-light-driven photocatalytic activity for degradation of RhB via a hydrothermal process and subsequent calcination [19]. 3D Bi_2O_3 hierarchical architectures assembled by 2D nanoplates were fabricated from electrodeposited bismuth (Bi) film, which exhibited a strong and wide photoluminescence signal [20]. More recently, Wang et al prepared 3D hierarchical flowerlike Bi_2O_3 microstructures composed of decahedrons and rods using a solution precipitation method with the assistance of glycerin [21]. Bouquet-like hierarchical Bi_2O_3 photocatalysts with high-density surface oxygen vacancy have been synthesized via a hydrothermal method by the synergetic control of NaOH and a polyvinyl alcohol (PVA) stabilizer [22].

Although various methods have been successfully used to synthesize Bi_2O_3 hierarchical architectures, the challenge has been remained to explore a simple synthetic route and understand formation mechanism to achieve the control. Room-temperature precipitation method is easy and economic for the preparation of Bi_2O_3 nanoparticles [23,24]. However, acid (HNO_3 or HCl) was

* Corresponding authors. Tel./fax: +86 25 84315054.
E-mail addresses: hanqiaofeng@njust.edu.cn (Q.-F. Han), wangx@njust.edu.cn (X. Wang).

http://dx.doi.org/10.1016/j.jallcom.2014.06.011
0925-8388/

usually used to inhibit hydrolysis of $Bi(NO_3)_3$ in order to control uniform precipitation, so extremely excess NaOH was added to neutralize the acid and obtain pure Bi_2O_3. Additionally, to the best of our knowledge, there is little report on the preparation of Bi_2O_3 hierarchitectures via a room precipitation method. Herein, by using DMF as a solvent to dissolve $Bi(NO_3)_3$, pure Bi_2O_3 microcrystallites in flowerlike shape assembled by nanobrick-based petals with pineapple surface were easily obtained at room temperature after 1 h of reaction. Moreover, the Bi_2O_3 crystals of different shapes including bundles and dendrites were obtained by varying the ratio of DMF/H_2O. The corresponding mechanism for the formation of various Bi_2O_3 architectures was proposed. Finally, the influence of Bi_2O_3 in various shapes on the photocatalytic activity for degradation of RhB under visible-light irradiation was investigated.

2. Experimental

A homogeneous solution of $Bi(NO_3)_3{\cdot}5H_2O$ (0.97 g, 2 mmol) in 25 mL DMF was added into saturated KOH/H_2O solution (5 mL distilled water, 5.0 g (89 mmol) KOH), and the solution changed pale yellow at once. The mixture was stirred for 3 min, and then left still and aging for about 1 h. The product was collected by filtration, washing several times with deionized water and ethanol, and drying at 60 °C for 12 h. No additional thermal treatment was needed.

The effect of the DMF/H_2O ratio on Bi_2O_3 morphologies was investigated. The detailed experimental results are listed in Table 1.

The X-ray diffraction patterns (XRD) were obtained on a Bruker D8 Advance X-ray diffractometer (Cu Kα radiation, λ = 1.5418 Å) at a scan rate of 0.05° 2θ s^{-1}. Transmission electron microscopy (TEM) and high-resolution TEM (HRTEM) were carried out on a JEM-2100 (JEOL) and FEI Tecnai T20 microscope equipped with an X-ray energy dispersive spectrometer (EDS), respectively. Field-emission scanning electron microscopy (FESEM) was performed on a HITACHI S-4800 microscope. A Quanta Chrome Nova 1000 analyzer was employed to measure the Brunauer–Emmett–Teller (BET) surface areas of the samples at liquid nitrogen temperature. X-ray photoelectron spectroscopy (XPS) measurements were carried out on a PHI Quantera II SXM X-ray photoelectron spectrometer with monochromatized Al Kα as the exciting source, and the results obtained in the XPS analysis were corrected by referencing the C 1s line to 284.8 eV. The UV–Vis diffuse reflectance spectra (DRS) of the products were determined on a Shimadzu UV 2550 spectrophotometer equipped with an integrating sphere, using $BaSO_4$ as a reference.

The photocatalytic activity of the Bi_2O_3 microcrystallites was evaluated by Rhodamine B (RhB) degradation. The Bi_2O_3 powders (0.05 g) were dispersed in 50 mL RhB aqueous solution (5 ppm) under continuous stirring, allowing 1 h in the dark to reach the adsorption–desorption equilibrium between RhB and Bi_2O_3 particles. Visible light irradiation using a xenon lamp (500 W) was applied to the suspension with continuous stirring. At a given time interval, about 5 mL of the suspension was taken out, the catalyst powders were removed by centrifugation, and residual concentration of the dye in the solution was obtained by using a UV–Vis spectrophotometer (BRAIC UV 1201).

3. Results and discussion

The purity of the product was strongly dependent on the ratio of [KOH]/[Bi]. When the [KOH]/[Bi] ratio was 89:2, phase pure α-Bi_2O_3 was obtained. As displayed in Fig. 1a, XRD pattern of the Bi_2O_3 microcrystallite obtained at DMF/H_2O ratio of 5:1 (**A1**) can be indexed to monoclinic α-Bi_2O_3 (JCPDS No. 41-1449). No peaks of impurities were detected, revealing the high purity of the product. The reflection peaks are strong and sharp, which indicates that as-prepared Bi_2O_3 was well crystalline. The XRD patterns of the samples **A2**–**A4** obtained at various DMF/H_2O ratios also correspond to pure α-Bi_2O_3 phase (Supporting Information Fig. S1). If the [KOH]/[Bi] ratio was decreased to 71:2, the XRD pattern revealed the presence of the impurity $BiONO_3$ (Fig. 1b), which suggests that sufficiently high ratio of [KOH]/[Bi] was necessary for the formation of phase pure Bi_2O_3, different from the result reported by Wu et al. [23].

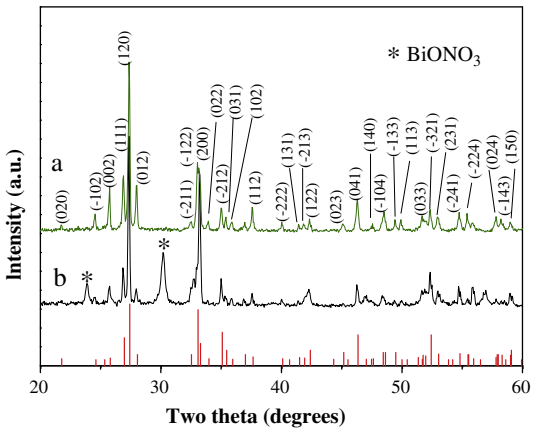

Fig. 1. XRD patterns of the as-prepared Bi_2O_3 microcrystallites: (a) [KOH]/Bi = 89/2 (**A1**) and (b) [KOH]/[Bi] = 71/2. Vertical sticks below the patterns represent the standard diffraction data from JCPDS file for bulk Bi_2O_3 with monoclinic structure (No. 41-1449).

A representative SEM image of the product **A1** is shown in Fig. 2a. The flower-like Bi_2O_3 hierarchical architectures contain multi-petals. These petals are aligned perpendicularly to the flower surface with clearly orientation, pointing toward a common center. The surfaces of petals were rough, analogous to pineapples. A high-magnification SEM image indicates that the pineapple-shaped petals were composed of nanobricks attached along certain direction, forming 1D structured petal (Fig. 2b). A TEM image of **A1** further confirms that the Bi_2O_3 microcrystallites were made up of several individual petals with the length of about 5 μm and diameter of 2–3 μm (Fig. 2c), and the edges of the petals look like zigzag stacks of nanobricks (inset in Fig. 2c). These nanobricks were too thick (~200 nm) to perform HRTEM studies.

The morphologies of Bi_2O_3 microcrystallites were obviously influenced by the ratio of DMF/H_2O. As shown in Fig. 2d, the flower-shaped Bi_2O_3 crystals (**A2**) made up of microrods with a diameter of about 1 μm were formed when the DMF/H_2O ratio was decreased to 2. With the amount of water increasing further ($V_{DMF/H2O}$ = 1), the rod-based Bi_2O_3 bundles (**A3**) with a rod size of about 200 nm in diameter and 20–40 μm in length were observed (inset in Fig. 2d). If using pure H_2O as solvent, typical TEM images indicate that the dendrite-shaped Bi_2O_3 microstructures (**A4**) consisted of dozens of nanorods with a diameter of about 80 nm extending radially from one root (Fig. 2e and its inset). An HRTEM image of a typical nanorod shows that the obtained Bi_2O_3 dendrites are highly crystalline (Fig. 2f). The measured lattices distance with *d*-spacings of 0.528, 0.331 and 0.276 nm corresponds to (011), (111), and ($\bar{2}$11) planes of α-Bi_2O_3, respectively. The selected area electron diffraction (SAED) patterns could be indexed to monoclinic structure with zone axis of [01$\bar{1}$] (upper left inset in Fig. 2f), which is consistent with the hexagonal lattice in the FFT diffractograms (lower right inset in Fig. 2f). The calculated zone axis and the fringes in the HRTEM image indicate that the Bi_2O_3 nanorods grow along the [001] orientation.

A time-dependent experiment was conducted to track the morphological evolution of the nanobrick-based flowerlike Bi_2O_3 microcrystallites (**A1**). When $Bi(NO_3)_3$/DMF solution was mixed

Table 1
DMF/H_2O ratio, morphologies, band gap energy and apparent rate constant *k* of RhB photodegradation.

Sample[a]	DMF/mL	H_2O/mL	Morphology	Bandgap/eV	k/h^{-1}
A1	25	5	Brick-based flowers	2.70	0.16
A2	20	10	Rod-based flowers	2.82	0.38
A3	15	15	Rod-based bundles	2.84	0.53
A4	0	30	Rod-based dendrites	2.88	0.63

[a] [KOH]/[Bi] = 89/2.